Cardiology in the Young 2011; Page 1 of 12
doi:10.1017/S1047951111001491

Original Article

Pulsatile venous waveform quality affects the conduit performance in functional and "failing" Fontan circulations

Onur Dur,[1] Ergin Kocyildirim,[2] Ozlem Soran,[3] Peter D. Wearden,[2] Victor O. Morell,[2] Curt G. DeGroff,[4] Kerem Pekkan[1,5]

[1]Department of Biomedical Engineering, Carnegie Mellon University; [2]Section of Pediatric Cardiothoracic Surgery of the Heart, Lung and Esophageal Surgical Institute, University of Pittsburgh Medical School, Children's Hospital of Pittsburgh; [3]Cardiovascular Institute, University of Pittsburgh, Pittsburgh, Pennsylvania; [4]Congenital Heart Center, University of Florida, Gainesville, Florida; [5]Department of Mechanical Engineering, Carnegie Mellon University, Pittsburgh, Pennsylvania, United States of America

Abstract *Objective:* To investigate the effect of pulsatility of venous flow waveform in the inferior and superior caval vessels on the performance of functional and "failing" Fontan patients based on two primary performance measures – the conduit power loss and the distribution of inferior caval flow (hepatic factors) to the lungs. *Methods:* Doppler angiography flows were acquired from two typical extra-cardiac conduit "failing" Fontan patients, aged 13 and 25 years, with ventricle dysfunction. Using computational fluid dynamics, haemodynamic efficiencies of "failing", functional, and *in vitro*-generated mechanically assisted venous flow waveforms were evaluated inside an idealised total cavopulmonary connection with a caval offset. To investigate the effect of venous pulsatility alone, cardiac output was normalised to 3 litres per minute in all cases. To quantify the pulsatile behaviour of venous flows, two new performance indices were suggested. *Results:* Variations in the pulsatile content of venous waveforms altered the conduit efficiency notably. High-frequency and low-amplitude oscillations lowered the pulsatile component of the power losses in "failing" Fontan flow waveforms. Owing to the offset geometry, hepatic flow distribution depended strongly on the ratio of time-dependent caval flows and the pulsatility content rather than mixing at the junction. "Failing" Fontan flow waveforms exhibited less balanced hepatic flow distribution to lungs. *Conclusions:* The haemodynamic efficiency of single-ventricle circulation depends strongly on the pulsatility of venous flow waveforms. The proposed performance indices can be calculated easily in the clinical setting in efforts to better quantify the energy efficiency of Fontan venous waveforms in pulsatile settings.

Keywords: "Failing" Fontan patient; congenital cardiac disease; pulsatility index; computational fluid dynamics; power loss; hepatic flow distribution

Received: 17 December 2010; Accepted: 17 July 2011

THE THIRD STAGE FOR PALLIATIVE SURGICAL reconstruction for children with functional single-ventricle physiology is the completion of the total cavopulmonary connection, where the superior and inferior caval vessels are routed directly into the pulmonary arteries.[1] This patient population continues to grow, with approximately 5000 newborns in the United States joining the existing single-ventricle patient population each year, along with increasing numbers of adult Fontan patients surviving longer because of the advances in surgical techniques and post-operative management. Although most post-operative Fontan patients experience an acceptable quality of life, their lifespan is shorter than normal, with a significant number of these patients developing

Correspondence to: Dr K. Pekkan, PhD, Assistant Professor, Biomedical Engineering Department, Carnegie Mellon University, 700 Technology Drive, Pittsburgh, Pennsylvania 15219, United States of America. Tel: 412 268 3027; Fax: 404 268 9807; E-mail: kpekkan@andrew.cmu.edu

late haemodynamic complications.[2,3] Unfortunately, for many Fontan patients, cardiac transplantation has now become their final "stage" option.

Following the single-ventricle palliation, there is increased afterload and decreased preload reserve in the Fontan circulation. This requires low pulmonary vascular resistance, which is associated with the calibre of the main pulmonary arteries and downstream vasculature, to alleviate the low cardiac output state.[4,5] Surgical pathway resistance is an integral piece of pulmonary vascular resistance, and in some functional patients it can be as high as the pulmonary vascular resistance, which would affect the cardiac output non-linearly, with further consequences at exercise.[6] Both our earlier *in vitro* physiological bioengineering models[7] and recent clinical studies[8,9] suggest that Fontan physiology necessitates vascular remodelling towards stiffer venous compliance to restore the normal cardiac output. The absence of direct ventricular assistance for pulmonary blood flow along with these altered venous characteristics suggests that optimisation of the Fontan pathway haemodynamics may improve patient outcomes. Most of the published efforts to date have focused on minimising energy losses within Fontan connections.[10–13] An extensive review of these studies has been provided by our group.[14] Efforts to quantify the steady-state energy losses inside patient-specific total cavopulmonary connection geometries[6,11,15] identified non-dimensional power-loss metrics that depend on steady-state pathway flow rate – cardiac output; patient body surface area – total cavopulmonary connection size; secondary anatomical features – offset, flare, etc.; and pulmonary flow split.[16] As demonstrated in this study, the non-dimensional formulation allows performing parametric studies, where the effect of a particular metric, that is, cavopulmonary flow pulsatility, can be investigated by fixing each other parameter, that is, cardiac output, flow splits, and surgical design dimensions.

Pulsatile flow simulations incorporating phase-contrast magnetic resonance image measurements have recently been used in pre-surgical planning applications.[17,18] *Nevertheless, limited attention has been given to the real-time "pulsatile" venous flow characteristics of the cavopulmonary pathway associated with the pronounced respiratory effects within the single-ventricle circulation.*[19] Our recent experimentally validated pulsatile computational investigations with real-time pulsatile caval waveforms suggest that for fixed cardiac output, energy loss is significantly influenced by the phase-angle between caval inflows.[20] This prompted the present study where the caval waveform topologies of "failing" Fontan patients are found to be considerably different from those found in functional Fontan patients. In addition, to our knowledge, the energy state in the "failing" Fontan group has not been well documented. On the basis of the theoretical advantage of minimising energy losses in the single-ventricle circuit, we hypothesise caval flow pulsatility to be a significant haemodynamic parameter among the other factors.[21] Similarly, the distribution of suspected "hepatic growth factors", which are thought to be carried by the inferior caval flow stream to the pulmonary arteries, needs to be investigated at pulsatile flow conditions. Quantification of the energy efficiency of the "failing" venous flows may provide additional haemodynamic indices that complement the previously derived steady total cavopulmonary connection energy loss formulations.[16]

The major causes of late mortality in this patient cohort have been attributed to impaired ventricular function, due to systemic right ventricle morphology;[22–25] low ejection fraction less than 60%;[22] atrioventricular valve regurgitation;[22] higher ventricular end-diastolic pressure;[23,24] protein-losing enteropathy;[24] thromboembolism;[24] elevated pulmonary artery pressures;[23] and atrial arrhythmias.[23] Modern non-invasive methods of *in vivo* investigation – such as phase-contrast magnetic resonance imaging, computational tomography, and modern echocardiography – are beginning to help improve the overall understanding of late Fontan failure. Results using such imaging techniques will be used here in efforts to better understand the effects of caval flow pulsatility.

Earlier bioengineering studies on Fontan haemodynamics exclusively focused on patients who are doing well, despite the growing number of adult late survivors with declining haemodynamic states. The available multi-channel acquisition of caval waveforms, respiratory and echocardiography signals reveal that the caval flow waveforms at rest are mainly based on two harmonics corresponding to respiratory and cardiac effects.[26,27] Real-time magnetic resonance imaging measurements by Hjortdal et al[19] in patients with total cavopulmonary connection (mean age: 12, standard deviation: 4.6) show that the inferior caval flow waveform is periodic, in phase with the echocardiography signal, and has a biphasic topology. For these functional single-ventricle patients, the flow variations in the inferior caval flow waveform coincide well with the respiratory cycle, and minimum flow appears close to the end of expiration. In contrast, the corresponding superior caval flow waveforms do not have a well-defined characteristic shape.[19] A comparison of both normal patients and single-ventricle patients (mean age: 10, standard deviation: 4) by Hsia et al[27] reported similar observations on caval waveforms but emphasised significantly lower cardiac dependence of caval flow in total cavopulmonary connection compared with normal patients. A recent magnetic resonance imaging study identified that patients with extra-cardiac conduit (mean age: 13.8, standard deviation: 11.2) and intra-atrial lateral tunnel (mean age: 16.9,

standard deviation: 11.6) have significantly less caval pulsatility compared with atriopulmonary connections (mean age: 19.0, standard deviation: 7.9).[28] The authors highlighted the suboptimal haemodynamic state, that is, retrograde flow and atrial dilation, of the atriopulmonary connection and speculate the utility of caval pulsatility evaluation to predict late Fontan failure.

On the basis of these investigations, the objective of this study was to quantify the characteristic venous flow pulsatility and associated changes in the surrogate measures of haemodynamic performance – energy efficiency and hepatic flow distribution – in "failing" and functional Fontan patients. We aim to focus on the sequel of altered venous flow pulsatility in order to suggest the potential causes for the suboptimal physiological state of the "failing" Fontan patient group.

Materials and methods

Patient selection and ultrasonographic caval flow waveforms

We chose two representative "failing" Fontan patients, aged 25 and 13 years, with severe suboptimal haemodynamics in the New York Heart Association functional class III. Formerly, both patients underwent an extra-cardiac total cavopulmonary connection procedure without employing fenestration and were examined 14 years (standard deviation: 7) after the operation for this study. Before the examination, "failing" Fontan-1 patient developed major pulmonary arteriovenous malformations; both patients had ventricle systolic dysfunction and abnormal sinus rhythm, yet no clinical signs of protein-losing enteropathy. The subjective assessment of ventricular systolic function by echocardiography indicated impairment, and magnetic resonance imaging assessment of the ejection fraction was not available. "Failing" Fontan caval waveforms were acquired in-house using multichannel simultaneous echocardiography, respiration, and real-time ultrasound measurements at the University of Pittsburgh, Children's Hospital. Measurements were recorded with an Acuson 128XP computed sonography (Acuson, Mountain View, California, USA), incorporating a 2.5-megahertz transducer during tidal breathing. Doppler sampling was guided via colour flow mapping to minimise the angle of insonation between the direction of the flow and the Doppler beam. Recordings were performed at the inferior caval vessel, 2 centimetres distal to the junction hepatic vein, and at the superior caval vessel, 1 centimetre distal to the junction to left pulmonary artery, for several respiratory cycles. Ultrasonic flow waveforms for the "failing" Fontan-2 patient (body surface area: 1.2 square metre, heart rate: 56 beats per minute, respiration rate: 32 cycles per minute) for three respiratory cycles is given in Figure 1. The corresponding functional Fontan caval waveforms were reproduced from the patient-specific real-time phase-contrast magnetic resonance imaging measurements available in the literature and are shown in Figure 2a.[19] The trial was approved by the institutional review boards of the University of Pittsburgh. Informed consent was obtained from all patients before study enrolment.

The effectiveness of the emerging mechanical assist therapies for single-ventricle patients[29,30] may be influenced by the caval flow waveform quality and its effect on the local total cavopulmonary connection haemodynamics. Hence, in addition to the patient-specific caval flows, the pulsatile haemodynamic efficiency of waveforms generated through Fontan mechanical circulatory support is also investigated. The mechanically assisted venous flow waveforms utilised in this study were acquired (Fig 2b) through the six-compartmental bench-top of pulsatile single-ventricle flow loop incorporating Medos pulsatile infant ventricle assist device (Medos Medizintechnik AG, Stolberg, Germany; SV: 10 millilitres, 100 beats per minute) anastomosed to the inferior caval vein.[31]

Flow waveform pulsatility analysis

Frequency and amplitude content of each caval flow waveform set was identified using fast Fourier transform, as shown in Figures 2 and 3. A discrete number of harmonics was used to reconstruct the time-dependent variation of venous flows, which is in strong agreement with the original ultrasound data ($R^2 = 0.90$). Reconstructed "failing" Fontan flow waveforms were scaled to match the mean cardiac output of the functional Fontan data ($Q = 3$ litres per minute) in order to allow an unbiased comparison of caval pulsatility-dependent power loss and hepatic flow distribution.

To quantify the pulsatility of the flow waveforms, two pulsatility indices were proposed. Time integral of the fluctuation of the total instantaneous venous flow, $Q_V(t)$ from the time-average caval flow rate Q_{AVG} – that is, total cardiac output = 3 litres per minute, constant for this study – provided an index to predict the energy loss increase due to any arbitrary pulsatile flow waveform. The Total Caval flow Pulsatility Index was defined as

$$\text{Total Caval flow Pulsatility Index} = \frac{1}{T}\int_0^T \left|\frac{Q_V(t)}{Q_{AVG}} - 1\right| dt \quad (1)$$

where $Q_V(t) = Q_{IVC}(t) + Q_{SVC}(t)$ and $Q_{AVG} = (1/T)\int_0^T Q_V(t)dt$. The caval flow waveforms appear periodic with a period, with T referring to the length of the respiration cycle.

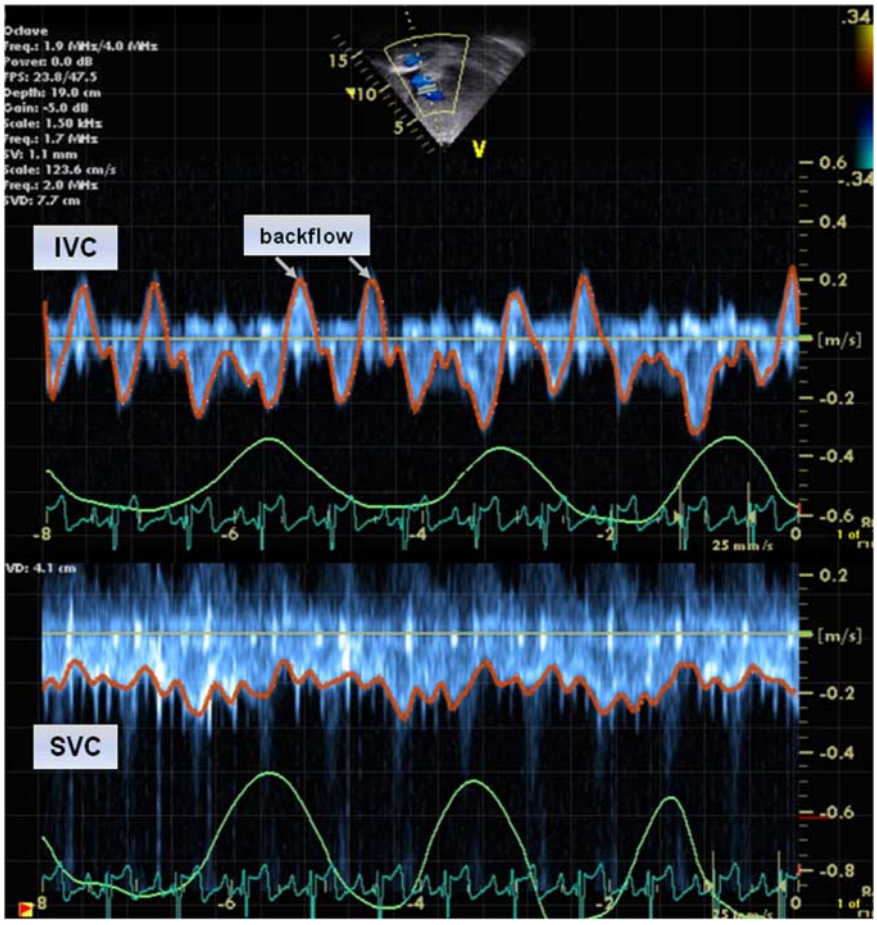

Figure 1.
Raw pulse-wave caval Doppler recordings sync with the respiration of the "failing" Fontan-2 patient. FF2 = "failing" Fontan-2 patient; IVC = inferior caval vein; SVC = superior caval vein.

Frequency content of the inflow waveforms were quantified by a second index, that is, the Caval Frequency Index, which averages the amplitude-weighted frequency of the major harmonics of the caval flow waveforms. The number of harmonics used to decompose venous waveforms, utilised in the caval frequency index calculation, was determined based on the desired accuracy of the waveform reconstruction ($R^2 = 0.90$):

$$\text{Caval Frequency Index} = \frac{1}{2}\left(\sum_{i=1}^{IVC} f_i A_i + \sum_{i=1}^{SVC} f_i A_i\right) \quad (2)$$

In the above formula, subscript f_i and A_i refer to the frequency and amplitude of the harmonics associated with inferior and superior caval flow waveforms. To further illustrate the influence of the caval flow pulsatility on the haemodynamic performance, the total amplitude fluctuations – that is, Total Caval flow Pulsatility Index – of the functional Fontan flow waveforms were minimised by modulating the phase-angle between the caval vein waveforms based on the protocol described previously.[20] These venous flow waveforms were named "optimal" and are shown in Table 1.

Computational fluid dynamics

Computational fluid dynamics simulations were conducted on the idealised one-diameter offset standard total cavopulmonary connection geometry in order to illustrate the isolated effect of flow waveform pulsatility on energy loss[20] and remove the anatomy bias. Computations were performed using the unsteady second-order accurate solver of FLUENT version 6.3.26 (ANSYS Inc., Canonsburg, Pennsylvania, United States of America) to simulate incompressible and Newtonian blood flow with constant haemodynamic properties ($\rho = 1060$ kilogram per cubic metre, $\mu = 3.71 \times 10^{-3}$ pascal-second).[10,20] The accuracy of the solver was validated experimentally using *in vitro* models.[10] Grid independency of the computational model (~250k computational elements)

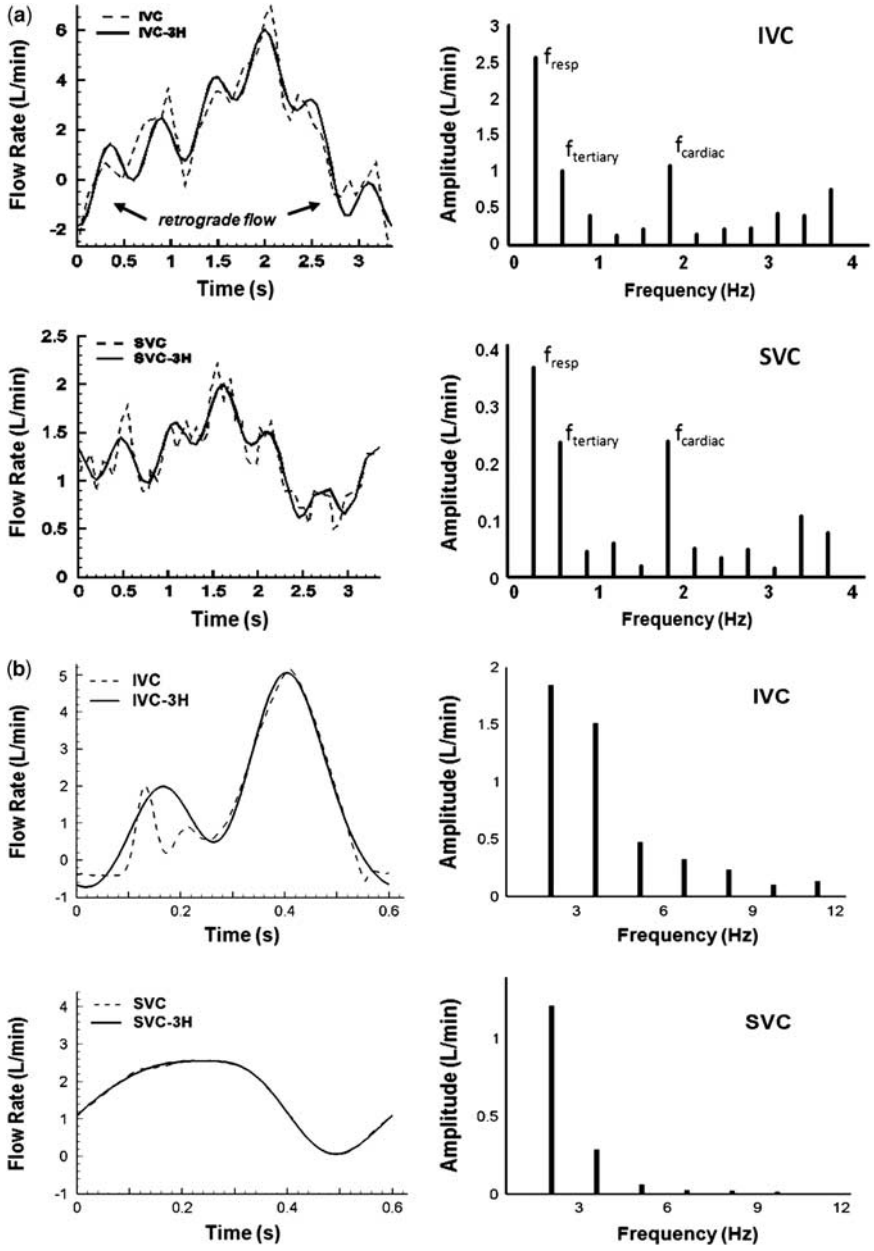

Figure 2.
*Real-time venous flow waveforms from a typical functional Fontan patient[19] (**a**) and the bench-top single-ventricle flow loop incorporating paediatric Medos ventricle assist device anastomosed to the inferior caval vein[31] (**b**) are plotted using three major harmonics over the original waveforms on the left. The frequency spectrum of each set of flow waveforms is given on the right. IVC = inferior caval vein; SVC = superior caval vein; 3H = three harmonics.*

was demonstrated previously.[20] Reconstructed cavopulmonary flow waveforms were specified as periodic inlet boundary conditions in the computational simulations. As higher flow rates are known to generate higher energy losses, that is, as in exercise,[6] to eliminate the effect of mean cardiac output all waveforms used are scaled to provide the same total cardiac output of 3 litres per minute. The energy loss inside the surgical connection was calculated on the basis of the energy difference between the inlet and outlets.[20] For the "failing" Fontan-1 patient, power loss is calculated through a converged running-average of three consecutive respiration cycles (~11 seconds) because of cycle-to-cycle variations (aperiodicity) in the caval flow waveforms. In contrast, the periodicity of caval flows synchronised with the respiratory cycle allowed evaluation of the power loss for "failing" Fontan-2 and functional Fontan patients based on one respiration cycle. Hepatic flow distribution to the lungs was calculated by computing the trajectories of 400–600

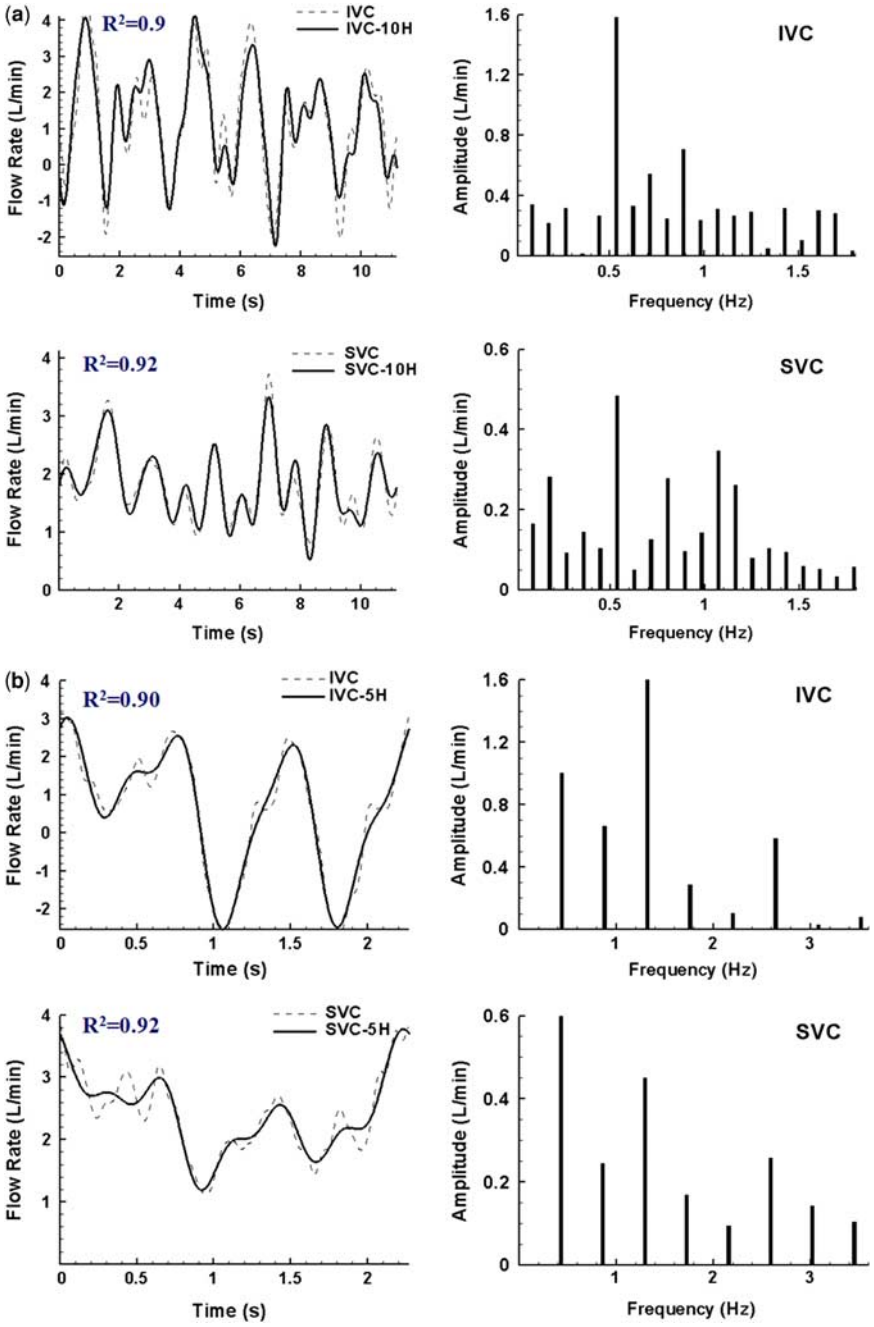

Figure 3.
*Doppler measurements of patient-specific "failing" caval flow waveforms (dashed lines) for "failing" Fontan-1 patient (**a**) and "failing" Fontan-2 patient (**b**) are reconstructed with discrete number of harmonic components (solid lines) with high accuracy ($R^2 = 0.90$). The full spectral decompositions of these waveforms are also provided on the right. IVC = inferior caval vein; SVC = superior caval vein; 5H = five harmonics.*

zero-mass particles seeded across the inferior caval vessel inlet.[32] Pulmonary flow split was adjusted to satisfy equal flow distribution ($Q_{LPA}/Q_{RPA} = 1$) to both lungs at each time step. The details of the computational model have been previously described by Dur et al[20] Scatter plots and statistical regression analysis were performed with MedCalc Software Version 11.4.4 (Mariakerke, Belgium) to assess the strength and significance of the correlations between power loss and pulsatility indices.

Results

Detailed spectral analysis indicated that the functional Fontan caval flow waveforms can be accurately reconstructed ($R^2 = 0.91$) using only the three main

Table 1. Summary of results for the conduit energy losses, echocardiography-derived parameters that describe the venous flow pulsatile characteristics, and the hepatic flow distribution to left pulmonary artery for the typical Fontan patient flow waveforms.

Flow waveform	Energy loss (mW)	TCPI (%)	CFI (rad/s)	$Q_{IVC}/Q_{SVC}(\beta)$	$Q_{H\text{-}LPA}/Q_{IVC}$ (%)
FUN	8.43	64	4.76	0.73	32
FF1	6.04	40	4.62	0.65	18
FF2	6.83	55	8.56	0.26	9
VAD	7.11	49	15.21	1.01	28
OPT	7.53	50	4.76	0.73	37

CFI = caval frequency index; FUN = functional Fontan patient; FF1 = "failing" Fontan-1 patient; FF2 = "failing" Fontan-2 patient; H-LPA = hepatic flow to left pulmonary artery; IVC = inferior caval vein; OPT = phase-angle-optimized Fontan flow waveforms; SVC = superior caval vein; TCPI = total caval flow pulsatility index; VAD = ventricle assist device

harmonics – the respiratory ($f_{resp} \sim 0.3$ hertz), cardiac ($f_{cardiac} \sim 1.8$ hertz), and tertiary ($f_{tertiary} \sim 0.6$ hertz) components as shown in Figure 2a-left. The tertiary component indicated the complex nature of the caval flows related to compliant vessel walls, splanchnic flow contribution, inertia of blood flow, and downstream wave reflections. In contrast, the frequency spectrum of both "failing" Fontan flow waveforms appeared more complex and required increased number of discrete harmonic pairs for accurate waveform construction. For "failing" Fontan-1 data, cardiac and tertiary components were replaced by a series of relatively smaller amplitude harmonics distributed over a large (0.6–1.2 hertz) frequency band. For "failing" Fontan-2 data, an additional high-frequency (~2.6 hertz) harmonic contributed highly to the caval flow. The period of the respiration cycle was about 3.2 seconds for the functional Fontan flow waveforms (~0.3 hertz), whereas the respiration cycle was relatively shorter for "failing" Fontan-1 (~0.44 hertz) and "failing" Fontan-2 (~0.53 hertz). Albeit the inferior caval flow of the failing" Fontan-2 data, the respiratory harmonic component contributed relatively highest to both inferior and superior caval flows. This indicates the functional respiratory flow augmentation in these "failing" Fontan patients. The ventricle assist device flow waveforms comprised very high-frequency oscillations (2–5 hertz) because of the lack of low-frequency respiration flow augmentation in the bench-top single-ventricle flow loop[31] and the elevated pump speed to achieve the desired venous flow augmentation. Hence, cardiac pulsations were overridden in the ventricle assist device venous flow waveforms.

The energy efficiency of functional and "failing" Fontan flow waveforms, computed from computational fluid dynamics simulations, is found to be significantly different regardless of having the same time-averaged flow rate ($Q_{IVC} + Q_{SVC}$). Energy loss inside the one-diameter offset cavopulmonary connection geometry for the functional caval flow waveforms was 8.43 milliwatts, whereas the energy loss for "failing" Fontan-1 and "failing" Fontan-2 waveforms was 6.04 and 6.83 milliwatts, respectively (Table 1). Hence, energy loss was attenuated, which in turn increased the energy efficiency of the venous circulation by about 20–30% in "failing" Fontan patients for the fixed surgical design at the same cardiac output. Similarly, energy losses within the ventricle assist device-connected Fontan conduit appeared to be 16% lower than the functional and approximately 10% higher than the "failing" Fontan cases at the same cardiac output.

The two pulsatility indices (Equations 1 and 2) for each waveform were calculated from echocardiography data, based on the spectral content of the caval flow waveforms, and are presented in Table 1, together with the corresponding time-averaged energy loss. The pulsatile fluctuation of the total venous flow – total cavopulmonary pulsatility index – appeared to be the highest (approximately 64%) for the functional caval flows. The total cavopulmonary pulsatility index for the "failing" Fontan-1 and "failing" Fontan-2 patients and ventricle assist device-supported venous flow waveforms was notably lower, that is, 40%, 55%, and 49%, respectively. Figure 4a demonstrates that the marginally significant correlation ($p = 0.052$) between total cavopulmonary pulsatility index and the observed time-averaged hydrodynamic power loss variations at fixed cardiac output. The caval frequency index indicated that "failing" Fontan-2 (approximately 8.6) had a higher frequency content compared with "failing" Fontan-1 and functional Fontan flow data, which had similar frequency content (approximately 4.7). As expected, ventricle assist device venous waveforms had a notably higher frequency content (15.2) compared with the patient-specific venous flows because of the high pump speed and the lack of respiration in the bench-top single-ventricle mock loop.[31] According to Figure 4b, the power loss variation correlated weakly ($p < 0.69$) with caval frequency index provided that the outliers (failing Fontan-1 patient and functional waveforms) with significantly different total caval pulsatility index are excluded. Therefore, caval frequency index was unable

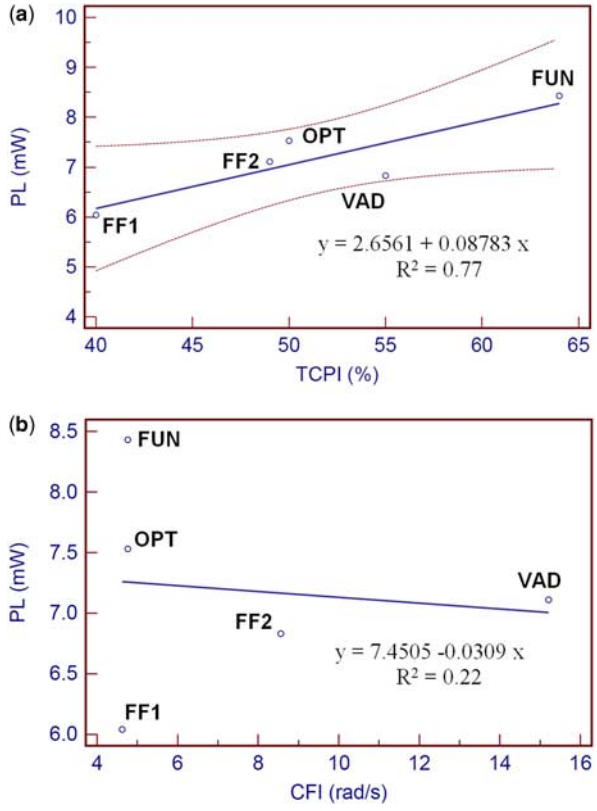

Figure 4.
*Total caval flow pulsatility index was correlated well ($p < 0.052$) with the observed time-averaged hydrodynamic power loss variations at fixed cardiac output and surgical connection (**a**). Power loss correlated weakly ($p < 0.69$) with caval frequency index (**b**). Dotted curves represent the 95% confidence interval for the regression line ($R^2 = 0.77$). CFI = caval frequency index; FF1 = "failing" Fontan-1 patient; FF2 = "failing" Fontan-2 patient; FUN = functional Fontan patient; OPT = phase-angle-optimized Fontan flow waveforms; PL = power loss; TCPI = total caval flow pulsatility index; VAD = ventricle assist device, respectively.*

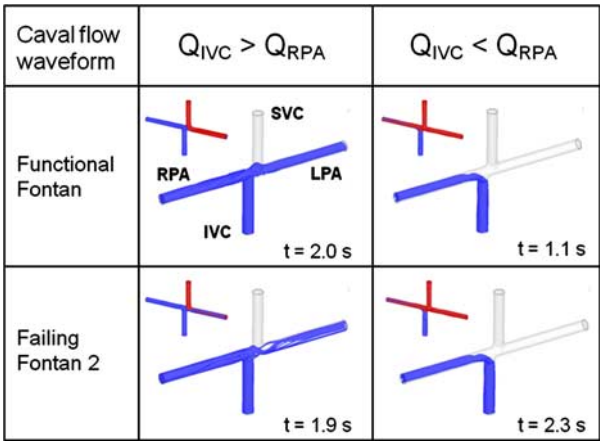

Figure 5.
Hepatic flow distribution for functional Fontan and "failing" Fontan 2 patient at two sets of representative time points during the respiration cycle, where inferior caval vein (blue) and superior caval vein (red) streams alternately dominate the flow distribution to the lungs. For the one-diameter offset total cavopulmonary connection geometry, hepatic flow distributes to the distal lung, left pulmonary artery, only when the flow reserve in the proximal lung is exceeded, that is, when inferior caval vein flow is higher than the right pulmonary artery flow. Note that for the particular case of $Q_{LPA}/Q_{RPA} = 1$, $Q_{IVC} > Q_{RPA}$ condition is analogous to $\beta = Q_{IVC}/Q_{SVC} > 1$ based on conversation of mass principle (net mass inflow = net mass outflow). IVC = inferior caval vein; LPA = left pulmonary artery; RPA = right pulmonary artery; SVC = superior caval vein.

to fully represent the variation in power loss for waveforms alone; instead, the pulsatile power loss was influenced by the interaction of multiple indices. The 'Discussion' section describes the collective interpretation of the pulsatile indices and their relation to the underlying physics.

Hepatic flow distribution between the lungs differed considerably both along the cardiac/respiration cycle and among the different caval flow waveforms, as shown in Table 1. Particle-flow tracking analysis indicated that inferior caval flow distributes to the distal lung only when the flow reserve in the proximal lung is exceeded, that is, when inferior caval flow exceeds the right pulmonary flow for the given one-diameter offset total cavopulmonary connection configuration (Fig 5). For the "failing" patients, only a limited portion of inferior caval flow (9–18%) was directed to the lung on the opposite side of the offset, that is, left pulmonary artery. Inferior caval flow was distributed more evenly for the functional Fontan (32%) and ventricle assist device (28%) flow waveforms (Table 1). Figure 6 shows the strong correlation ($p < 0.02$) between the hepatic flow reaching to the distal lung (Q_{H-LPA}/Q_{IVC}) and caval flow split ratio ($\beta = Q_{IVC}/Q_{SVC}$). This trend indicates that a more balanced inferior caval flow distribution was achieved when time-averaged inferior caval flow exceeds the superior caval flow, that is, higher β. In addition, comparing the functional and caval phase-angle-optimised flow waveforms[20] (details are presented in the 'Discussion' section), the flow distribution to the left pulmonary artery was further improved (approximately 15%) by optimising the pulsatile content of the caval flows at the fixed β.

Discussion

The Fontan operation is now a very common palliative procedure performed to treat patients with complex congenital cardiac defects unable to receive bi-ventricular repair. The Fontan procedure has created a growing population of patients with complex congenital cardiac disease, a significant

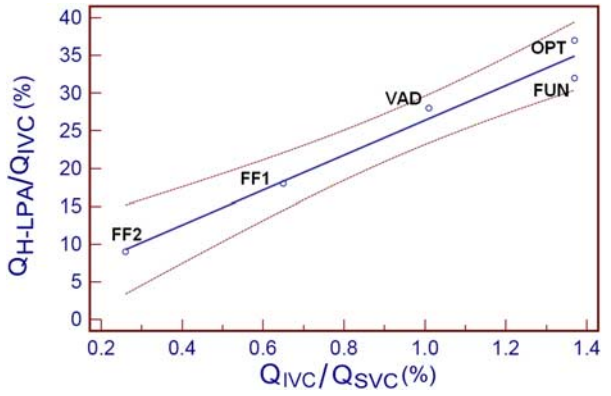

Figure 6.
Hepatic flow reaching the distal lung ($Q_{H\text{-}LPA}/Q_{IVC}$) correlated strongly ($p < 0.02$) with the caval flow split ratio ($\beta = Q_{IVC}/Q_{SVC}$). Dotted curves represent the 95% confidence interval for the regression line ($R^2 = 0.77$). FF1 = "failing" Fontan-1 patient; FF2 = "failing" Fontan-2 patient; FUN = functional Fontan patient; OPT = phase-angle-optimized Fontan flow waveforms; VAD = ventricle assist device; IVC = inferior caval vein; SVC = superior caval vein; H-LPA = hepatic flow to left pulmonary artery, respectively.

portion of who now survive past childhood. In fact, many of these Fontan patients now survive for decades, and much of the improved survival rates may be attributable to an improved understanding of Fontan haemodynamics leading to refined surgical procedures. The prospect of continuing late attrition, however, remains a genuine concern.

Unfortunately, progress to develop alternative surgical strategies for patients with single-ventricle physiology has been reaching a plateau with little derived physiological benefit from what are now minimal adjustments to already refined surgical techniques. Recent studies indicate that application of a paediatric mechanical circulatory support in the Fontan circuit may augment venous flow, improve ventricular preload, and reverse the Fontan Paradox of under-filling of the pulmonary arteries during late failing states of the disease.[30,31] However, poorly designed circulatory assist therapies could potentially increase caval flow stream collisions, resulting in poor conduit flow quality and worsening efficiencies. Therefore, such circulation assist options should be validated through clinical investigations guided by bioengineering analysis.[5,7,31]

Previously, we studied the pulsatile characteristics of venous flow waveforms that might be generated at the inferior and superior caval vessels by such venous assist therapies. Our numerical findings indicated that flow pulsatility variations due to the modulation of phase-angle between inferior and superior caval flow have a significant impact on venous energetics, and if optimised may provide 2–34% power loss relief – a function of conduit anatomy – inside the total cavopulmonary connection pathway for the fixed geometry.[20] By modulating the caval vein phase-angle, in turn decreasing the total caval pulsatility index, we demonstrated the feasibility of venous flow waveform optimisation, which yielded 11% lower energy loss compared with the functional data for the same cardiac output – 3 litres per minute. In this study, we embarked upon evaluating the venous flow energetics of the functional and "failing" Fontan patients based on the respiration-synchronised patient-specific Doppler ultrasound caval flow waveforms from a small subset of Fontan patients. Our computational study revealed that pulsatile energy loss of "failing" Fontan patient flow waveforms was significantly lower compared with the functional Fontan patient flow waveforms for the same cardiac output and fixed surgical template. Provided that the effect of cavopulmonary power loss on cardiac index is significant, having lower energy losses at this suboptimal state may be an intrinsic physiologic attempt to augment cardiac output in "failing" Fontan patients.[4,5] To note, it is faulty to interpret our findings, as the patient-specific "failing" Fontan energy efficiency is superior to the functional. Fully patient-specific energy evaluation of cavopulmonary power loss depends strongly on the cardiac output,[6,16] conduit geometry,[11,33,34] body surface area,[16] pulmonary anatomy,[4] and pulsatile content of the venous flow.[20] In this proof-of-concept study, we demonstrated the significance of patient-specific venous flow pulsatility on haemodynamic performance of Fontan connection and the higher efficiency of "failing" Fontan caval flows relative to the functional Fontan solely based on isolated effect of the pulsatile content, that is, for the same cavopulmonary geometry, body surface area and cardiac output.

The proposed echocardiography-derived pulsatility indices successfully predicted the energy efficiency of different caval flow waveform sets with different harmonic contents. Our results show that the total caval pulsatility index followed the trend in energy loss variation closely and provided a comparative basis for the venous energy efficiency in Fontan patients. On the other hand, a comparison between optimal and ventricle assist device flow waveforms indicated that, based on the higher frequency content, mechanically supported Fontan caval flow yielded lower power loss (6%) at the same total caval pulsatility index. Hence, in addition to the venous flow phase-angle and amplitude fluctuations, the frequency content of caval flow waveforms also influences the conduit energy efficiency remarkably. Recently, we developed a hybrid theoretical–numerical model and identified an analytical relationship between the pulsatile venous flow fluctuations and the energy loss inside total cavopulmonary connection.[35,36] These

analyses also indicated that the flow field within the one-diameter offset total cavopulmonary connection geometry follows the frequency-dependent characteristics of Womersley flow closely. Flow over a wide range of inflow frequency showed that the flow profile at low frequencies displayed a Poiseuille-like parabolic appearance along the one-diameter offset total cavopulmonary connection pathway. In contrast, when high-frequency oscillations were present, flow profiles were not able to reach the fully developed shape and yielded lower shear stresses, and in turn lower energy losses. Hence, higher frequency content of the "failing" Fontan-2 flow waveform contributed to the higher energy efficiency and agreed with our energy loss calculation. It is worthwhile to note that uneven caval flow split ($\beta \neq 1$) also affect the pathway power loss at fixed cardiac output,[12] and needs to be considered to fully identify the relation between caval pulsatility and energy losses.

Clinically, it will be valuable to delineate easy-to-calculate pulsatility parameters that can correlate with the conduit energetics and allow patient-to-patient comparisons. The proposed indices complement the previously introduced steady-state non-dimensional metrics to characterise the total cavopulmonary connection power losses[16] and allows predicting the pulsatile power loss changes without time-demanding in silico computational fluid dynamics calculations. This study suggests a retrospective protocol, where the time-resolved inferior and superior caval flows – if available also the pulmonary flows – are acquired and exported to a spreadsheet to calculate the proposed time-integral-based caval flow pulsatility indices. In addition, fast Fourier transform analysis is required to calculate the proposed frequency content index. This methodology can also be interfaced with any real-time imaging modality – Doppler Ultrasound or Magnetic Resonance Imaging – which will be particularly useful for comparing the pulsatile performance of any arbitrary Fontan patient venous flows for immediate feedback in clinic. To note, previously, several imaging-based pulsatility indices have been proposed as clinically meaningful parameters to assess the peripheral vascular disease and atherosclerotic occlusions, renovascular function, foetal cardiovascular function, and arterial growth.[37–39] Analogously, the proposed venous flow pulsatility indices may also provide a rationale that can correlate Fontan haemodynamics with altered cardiopulmonary dynamics, cardiac malfunction, and post-operative complications.[2,3] It is worthwhile to note that all the above image-based pulsatility indices, $PI = (Q_{max} - Q_{min})/Q_{mean}$, were used for quantifying the pulsatility of arterial flow waveforms with a characteristic monophasic topology synchronised with QRS complex. For the caval venous flow waveforms with biphasic or more complex topology, as in "failing" Fontan patients, traditional pulsatility index formulation may produce misleading results. A comparison of the proposed time-integral approach and traditional pulsatility index indicated that six out of twelve Fontan cavopulmonary flow waveforms fall outside of the correlation with 95% confidence interval (Fig 7). In addition, comparing the relative pulsatile content between the selected cavopulmonary waveforms (Table 2), the traditional pulsatility formula predicted relative pulsatility variation up to 70% error in comparison to the time-integral pulsatility scores. Hence, our study also demonstrates the significance of using the time-integral approach to quantify the cavopulmonary pulsatility in Fontan patients.

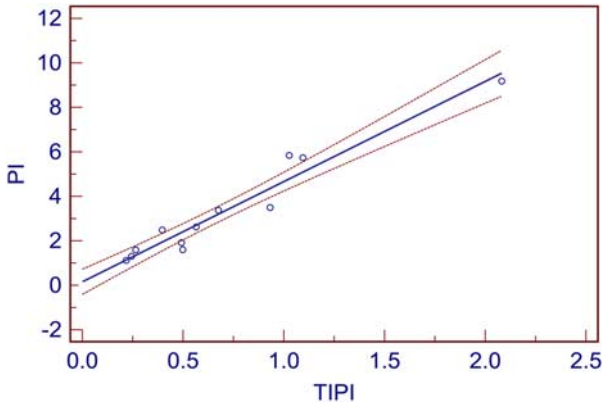

Figure 7.
Comparison of the proposed time-integral evaluation of pulsatility index, $TIPI = \frac{1}{T}\int_0^T \left|\frac{Q(t)}{Q_{mean}} - 1\right| dt$, and traditional pulsatility index, $PI = (Q_{peak} - Q_{min})/Q_{mean}$, indicated six out of twelve Fontan cavopulmonary flow waveforms fall outside of the correlation ($R^2 = 0.81$) with 95% confidence interval (dotted curves). Traditional pulsatility formula predicted the relative pulsatility variation between the given cavopulmonary waveforms with up to 70% error in comparison to the time-integral pulsatility scores. Q_{max}, Q_{min} and $Q_{mean} = \frac{1}{T}\int_0^T Q(t)dt$, refer to the instantaneous flow waveform, peak flow, minimum flow and time-averaged flow, and period of the flow waveform, respectively. PI = pulsatility index; TIPI = time-integral evaluation of pulsatility index.

Recent clinical studies indicate that liver-derived "hepatic factors" are required for prevention of the pulmonary arteriovenous malformations,[40] and thus to allow normal lung development. Even distribution of hepatic flow to the lungs will ensure sustaining adequate concentration of hepatic factors present in the lungs. Hepatic flow distribution depends strongly on the surgical design of the cavopulmonary conduit.[32] Theoretically, for the one-diameter offset total cavopulmonary connection geometry, which offers minimum cross-flow mixing at the cavopulmonary junction, the relative hepatic flow reaching the lungs will depend solely on the inferior caval vein flow split

Table 2. Pulsatility indices evaluation for the four cavopulmonary flow waveform sets based on traditional PI and TIPI formulations.

Flow waveform	PI	TIPI
FUN		
IVC	5.7	1.1
SVC	1.3	0.2
PA	3.4	0.7
FF1		
IVC	5.8	1.0
SVC	1.6	0.3
PA	2.5	0.4
FF2		
IVC	9.2	2.1
SVC	1.1	0.2
PA	2.6	0.6
VAD		
IVC	3.5	0.9
SVC	1.6	0.5
PA	1.9	0.5

FUN = functional Fontan patient; FF1 = "failing" Fontan-1 patient; FF2 = "failing" Fontan-2 patient; IVC = inferior caval vein; PA = pulmonary artery; PI = pulsatility index; SVC = superior caval vein; TIPI = time integral pulsatility index; VAD = ventricle assist device
Similar to the total cavopulmonary pulsatility index, time integral pulsatility index is calculated as $TIPI = \frac{1}{T}\int_0^T \left|\frac{Q(t)}{Q_{mean}} - 1\right| dt$, whereas, traditional pulsatility index is defined as $PI = (Q_{max} - Q_{min})/Q_{mean}$. $Q(t)$, Q_{max}, Q_{min}, and $Q_{mean} = \frac{1}{T}\int_0^T Q(t)dt$, refer to the instantaneous flow waveform, peak flow, minimum flow and time-averaged flow and period of the flow waveform, respectively

to lungs. Our analysis indicated that for the fixed cardiac output and one-diameter offset surgical connection, inferior caval flow distribution to lungs depends strongly on the patient-specific caval flow waveforms. On the basis of the superior caval flow dominance, that is, lower β, "failing" Fontan patients exhibited compromised hepatic flow distribution to their lungs – to the lung distal to inferior caval vessel anastomosis. Comparison of the functional and caval phase-angle-optimised flow waveforms – at the same β – highlighted the effect of pulsatility on the hepatic flow distribution within the one-diameter offset total cavopulmonary connection. Hence, we demonstrated that modulation of the caval phase-angle not only reduces the hydrodynamic energy losses within the one-diameter offset total cavopulmonary connection,[20] but also allows the inferior caval flow to distribute more evenly between the lungs. Hepatic flow distribution and its relation to "β and flow pulsatility" for different offset designs require further investigation. At present, this case study was based on a small patient cohort and lacks the effect of patient-specific anatomical features on venous pulsatility and compliance, which complicates the hepatic flow control. Therefore, this methodology needs to be expanded on a larger patient cohort, incorporate patient-specific anatomy, and post-operative haemodynamics in order to fully characterise the Fontan venous pulsatility and its correlation to the broader spectrum of "failing" Fontans.

The significant effect of caval pulsatility on cavopulmonary power dissipation may provide the impetus to design emerging mechanical assist therapies for single-ventricle patients to consider the influence of caval flow waveform quality on the local pathway haemodynamics. As a limitation, the ventricle assist device-inserted bench-top Fontan mock circuit lacked the sophistication of incorporating realistic respiratory mechanics and cardiothoracic interactions of the single-ventricle circulation. Possible animal models, more reliable bench-top paediatric single-ventricle flow loops, and circuit analogue lumped parameter models, are required for systemic evaluation and optimisation of new mechanical support strategies for short- or moderate-term use in the "failing" Fontans to decrease the workload on the single ventricle, thereby theoretically extending the life of the ventricle, or allow time as a bridge to transplant.[7,31]

Conclusion

This proof-of-concept study presents, to our knowledge, the first attempt to systematically quantify the haemodynamics in "failing" Fontan patients. On the basis of both the patient-specific Doppler echocardiography and mechanically generated time-resolved venous flows, we demonstrated the significance of venous flow pulsatility on conduit energetics and hepatic flow distribution within the one-diameter offset total cavopulmonary connection geometry. Our analysis indicated that because of the higher frequency content and lower amplitude fluctuations, "failing" Fontan patients had lower pulsatile energy dissipation, and in turn higher haemodynamic efficiency compared with the functional patients at the same normalised cardiac output. This lower pulsatile energy loss state for "failing" Fontan patients may be an indication of an inherent cardio/venous-adaptive management in order to reduce the strain on the malfunctioning single ventricle. Future numerical and *in vivo* studies will look to identify this condition incorporating a larger Fontan clinical database. As demonstrated in this study, quantification of the energy efficiency of the venous flow topology in terms of "clinically accessible" time-integral-based pulsatility indices may enable patient-to-patient haemodynamic performance comparison in clinic.

References

1. de Leval MR, Kilner P, Gewillig M, Bull C. Total cavopulmonary connection: a logical alternative to atriopulmonary connection for complex Fontan operations. Experimental studies and early clinical experience. J Thorac Cardiovasc Surg 1988; 96: 682–695.

2. Ghanayem NS, Berger S, Tweddell JS. Medical management of the failing Fontan. Pediatr Cardiol 2007; 28: 465–471.
3. Anderson PA, Sleeper LA, Mahony L, et al. Contemporary outcomes after the Fontan procedure: a Pediatric Heart Network multicenter study. J Am Coll Cardiol 2008; 52: 85–98.
4. Dasi LP, Krishnankuttyrema R, Kitajima HD, et al. Fontan hemodynamics: importance of pulmonary artery diameter. J Thorac Cardiovasc Surg 2009; 137: 560–564.
5. Sundareswaran KS, Pekkan K, Dasi LP, et al. The total cavopulmonary connection resistance: a significant impact on single ventricle hemodynamics at rest and exercise. Am J Physiol Heart Circ Physiol 2008; 295: H2427–H2435.
6. Whitehead KK, Pekkan K, Kitajima HD, Paridon SM, Yoganathan AP, Fogel MA. Nonlinear power loss during exercise in single-ventricle patients after the Fontan: insights from computational fluid dynamics. Circulation 2007; 116 (Suppl. 11): I165–I171.
7. Pekkan K, Frakes D, De Zelicourt D, Lucas CW, Parks WJ, Yoganathan AP. Coupling pediatric ventricle assist devices to the Fontan circulation: simulations with a lumped-parameter model. ASAIO J 2005; 51: 618–628.
8. Krishnan US, Taneja I, Gewitz M, Young R, Stewart J. Peripheral vascular adaptation and orthostatic tolerance in Fontan physiology. Circulation 2009; 120: 1775–1783.
9. Myers CD, Ballman K, Riegle LE, Mattix KD, Litwak K, Rodefeld MD. Mechanisms of systemic adaptation to univentricular Fontan conversion. J Thorac Cardiovasc Surg 2010; 140: 850–856.e6.
10. Wang C, Pekkan K, de Zelicourt D, et al. Progress in the CFD modeling of flow instabilities in anatomical total cavopulmonary connections. Ann Biomed Eng 2007; 35: 1840–1856.
11. Pekkan K, de Zelicourt D, Ge L, et al. Physics-driven CFD modeling of complex anatomical cardiovascular flows – a TCPC case study. Ann Biomed Eng 2005; 33: 284–300.
12. Khunatorn Y, Mahalingam S, DeGroff CG, Shandas R. Influence of connection geometry and SVC–IVC flow rate ratio on flow structures within the total cavopulmonary connection: a numerical study. J Biomech Eng 2002; 124: 364–377.
13. Bove EL, de Leval MR, Migliavacca F, Guadagni G, Dubini G. Computational fluid dynamics in the evaluation of hemodynamic performance of cavopulmonary connections after the Norwood procedure for hypoplastic left heart syndrome. J Thorac Cardiovasc Surg 2003; 126: 1040–1047.
14. DeGroff CG. Modeling the Fontan circulation: where we are and where we need to go. Pediatr Cardiol 2008; 29: 3–12.
15. Pekkan K, Kitajima HD, de Zelicourt D, et al. Total cavopulmonary connection flow with functional left pulmonary artery stenosis: angioplasty and fenestration in vitro. Circulation 2005; 112: 3264–3271.
16. Dasi LP, Pekkan K, Katajima HD, Yoganathan AP. Functional analysis of Fontan energy dissipation. J Biomech 2008; 41: 2246–2252.
17. Marsden AL, Reddy VM, Shadden SC, Chan FP, Taylor CA, Feinstein JA. A new multiparameter approach to computational simulation for Fontan assessment and redesign. Congenit Heart Dis 2010; 5: 104–117.
18. Sundareswaran KS, de Zelicourt D, Sharma S, et al. Correction of pulmonary arteriovenous malformation using image-based surgical planning. JACC Cardiovasc Imaging 2009; 2: 1024–1030.
19. Hjortdal VE, Emmertsen K, Stenbog E, et al. Effects of exercise and respiration on blood flow in total cavopulmonary connection: a real-time magnetic resonance flow study. Circulation 2003; 108: 1227–1231.
20. Dur O, DeGroff GC, Keller BB, Pekkan K. Optimization of inflow waveform phase-difference for minimized total cavopulmonary power loss. J Biomech Eng 2010; 132: 031012 (9 pages).
21. Dasi L, Sundareswaran K, Zelicourt D, et al. Fontan hemodynamics: what is the problem? JTCVS 2010; 139: 1673–1674.
22. Yoshimura N, Yamaguchi M, Oshima Y, et al. Risk factors influencing early and late mortality after total cavopulmonary connection. Eur J Cardiothorac Surg 2001; 20: 598–602.
23. Williams IA, Sleeper LA, Colan SD, et al. Functional state following the Fontan procedure. Cardiol Young 2009; 19: 320–330.
24. Khairy P, Fernandes SM, Mayer JE Jr, et al. Long-term survival, modes of death, and predictors of mortality in patients with Fontan surgery. Circulation 2008; 117: 85–92.
25. Hosein RB, Clarke AJ, McGuirk SP, et al. Factors influencing early and late outcome following the Fontan procedure in the current era. The 'Two Commandments'? Eur J Cardiothorac Surg 2007; 31: 344–352, discussion 353.
26. Marsden AL, Vignon-Clementel IE, Chan FP, Feinstein JA, Taylor CA. Effects of exercise and respiration on hemodynamic efficiency in CFD simulations of the total cavopulmonary connection. Ann Biomed Eng 2007; 35: 250–263.
27. Hsia TY, Khambadkone S, Redington AN, Migliavacca F, Deanfield JE, de Leval MR. Effects of respiration and gravity on infradiaphragmatic venous flow in normal and Fontan patients. Circulation 2000; 102 (19 Suppl. 3): III148–III153.
28. Klimes K, Abdul-Khaliq H, Ovroutski S, et al. Pulmonary and caval blood flow patterns in patients with intracardiac and extracardiac Fontan: a magnetic resonance study. Clin Res Cardiol 2007; 96: 160–167.
29. Pekkan K, Sasmazel A, Sundareswaran K, et al. Respiratory augmentation of blood flow in the early post-op Fontan circulation – feasibility of intra-pulmonic balloon pumping and external counterpulsation of systemic venous return. 16th World Congress of the World Society of Cardio-Thoracic Surgeons, Ottawa, Canada, 2006.
30. Throckmorton AL, Ballman KK, Myers CD, Frankel SH, Brown JW, Rodefeld MD. Performance of a 3-bladed propeller pump to provide cavopulmonary assist in the failing Fontan circulation. Ann Thorac Surg 2008; 86: 1343–1347.
31. Dur O, Lara M, Arnold D, et al. Pulsatile in vitro simulation of the pediatric univentricular circulation for evaluation of cardiopulmonary assist scenarios. Artif Organs 2009; 33: 967–976.
32. Dasi LP, Whitehead K, Pekkan K, et al. Pulmonary hepatic flow distribution in total cavopulmonary connections: extracardiac versus intracardiac. J Thorac Cardiovasc Surg 2011; 141: 207–214.
33. Marsden AL, Bernstein AJ, Reddy VM, et al. Evaluation of a novel Y-shaped extracardiac Fontan baffle using computational fluid dynamics. J Thorac Cardiovasc Surg 2009; 137: 394–403, e392.
34. Migliavacca F, Dubini G, Bove EL, de Leval MR. Computational fluid dynamics simulations in realistic 3-D geometries of the total cavopulmonary anastomosis: the influence of the inferior caval anastomosis. J Biomech Eng 2003; 125: 805–813.
35. Dur O. Investigation of the Unsteady Venous Hemodynamics in Fontan Patients to Enable New Therapeutic Options for Improving the Long Term Outcome. Biomedical Engineering, Carnegie Mellon University, Pittsburgh, 2011.
36. Dur O, Kocyildirim E, Degroff CG, Wearden P, Morell V, Pekkan K. Effect of caval waveform on energy dissipation of failing Fontan patients. Paper presented at: Proceedings of the ASME Summer Bioengineering Conference, Lake Tahoe, 2009.
37. Guyton JR, Hartley CJ. Flow restriction of one carotid artery in juvenile rats inhibits growth of arterial diameter. Am J Physiol 1985; 248 (4 Pt 2): H540–H546.
38. Ghabili K, Khosroshahi HT, Shakeri A, Tubbs RS, Bahluli A, Shoja MM. Can Doppler ultrasonographic indices of the renal artery predict the presence of supernumerary renal arteries? Transplant Proc 2009; 41: 2731–2733.
39. Evans DH, Barrie WW, Asher MJ, Bentley S, Bell PR. The relationship between ultrasonic pulsatility index and proximal arterial stenosis in a canine model. Circ Res 1980; 46: 470–475.
40. Justino H, Benson LN, Freedom RM. Development of unilateral pulmonary arteriovenous malformations due to unequal distribution of hepatic venous flow. Circulation 2001; 103: E39–E40.